

UNIVERSITY OF KWAZULU-NATAL (HOWARD COLLEGE)

MASTERS THESIS

Discrete Energy Minimisation Optimisation using Graph Cuts for Fluorescence Microscopy

Author:
Ryan NAIDOO

Supervisor:
Dr. Jules-Raymond TAPAMO

*A thesis submitted in fulfillment of the requirements
for the degree of Master of Science in Engineering*

in the

Department of Electrical, Electronic and Computer Engineering
School of Engineering

October 23, 2016

Declaration of Authorship

I, Ryan NAIDOO, declare that this thesis titled, “Discrete Energy Minimisation Optimisation using Graph Cuts for Fluorescence Microscopy” and the work presented in it are my own. I confirm that:

- This work was done wholly or mainly while in candidature for a research degree at this University.
- Where any part of this thesis has previously been submitted for a degree or any other qualification at this University or any other institution, this has been clearly stated.
- Where I have consulted the published work of others, this is always clearly attributed.
- Where I have quoted from the work of others, the source is always given. With the exception of such quotations, this thesis is entirely my own work.
- I have acknowledged all main sources of help.
- Where the thesis is based on work done by myself jointly with others, I have made clear exactly what was done by others and what I have contributed myself.

Signed:

Date:

"Thanks to my solid academic training, today I can write hundreds of words on virtually any topic without possessing a shred of information, which is how I got a good job in journalism."

Dave Barry

UNIVERSITY OF KWAZULU-NATAL (HOWARD COLLEGE)

Abstract

Faculty of Engineering
School of Engineering

Master of Science in Engineering

**Discrete Energy Minimisation Optimisation using Graph Cuts for Fluorescence
Microscopy**

by Ryan NAIDOO

The Thesis Abstract is written here (and usually kept to just this page). The page is kept centered vertically so can expand into the blank space above the title too...

Acknowledgements

The acknowledgments and the people to thank go here, don't forget to include your project advisor...

Contents

Declaration of Authorship	iii
Abstract	vii
Acknowledgements	ix
List of Figures	xiii
List of Tables	xv
List of Abbreviations	xix
1 Introduction	1
1.1 Literature Review	1
1.2 Outline and Contributions	1
1.3 Thesis Overview	1
2 Parameter Estimation for ACWE Chan-Vese Segmentation	3
2.1 Graph Cut Model for Chan-Vese Segmentation	3
2.2 Modified Weighting and Parameter Estimation	6
2.2.1 Graph Weighting	6
2.2.2 Analysis of Weighting System and Parameter Relationships	6
2.2.3 Tuning Parameters for Fluorescence Microscopy	10
2.3 Experimental Results	10
A Introduction to Graph Theory	11
B Cell Images Dataset	15
B.1 Test Data	15
Bibliography	21

List of Figures

2.1	(a) Cauchy-Crofton length approximation. (b) 8-connected neighbourhood system.	5
2.2	Fully connected single node.	6
2.3	Data energy functions plot.	8
2.4	Relationship between α and p_e	8
A.1	Undirected weighted graph G . The degree of each node is shown next to the corresponding node. The graph is simple. The red box shows the vertex set, V_G , and edge set, E_G , and their corresponding norm.	11
A.2	Directed weighted graph (Digraph) D . The in-degree and out-degree is shown next to each node. The graph is simple and not balanced. The red box shows the vertex set, V_D , and edge set, E_D , and their corresponding norm.	12
A.3	Undirected weighted graph H is a subgraph of G in Figure XX, $\mathbf{H} \subseteq \mathbf{G}$. Directed weighted graph I is a subgraph of D in Figure XX, $\mathbf{I} \subseteq \mathbf{D}$. The degree of each node is shown next to the corresponding node. The red box shows the vertex set, the edge set and their corresponding norms.	13
A.4	Cliques of the undirected weighted graph G . The maximal cliques are shown by the hyperedges that encompass the nodes of that clique.	13
B.1	Uneven Illumination	15
B.2	High cell density	15
B.3	Multi-modal (non-bi-modal)	16
B.4	Hazy/Glowing Edges	17
B.5	Thin Tentacles	18
B.6	Bright Spots and Speckles	19
B.7	To be categorised	20

List of Tables

List of Algorithms

List of Abbreviations

ACWE	Active Contours Without Edges
AOD	Average Optical Density
BCC	Boundary Chain Code
BFS	Breadth First Search
BP	Belief Propagation
CCD	Charge-Coupled Device
CED	Coherence Enhancing Diffusion
CLSM	Confocal Laser Scanning Microscopy
CRF	Conditional Random Field
DCC	Differential Chain Code
DFS	Depth First Search
DNA	Deoxyribonucleic Acid
DP	Dynamic Programming
DT	Delaunay Triangulation
EGFP	Enhanced Green Fluorescent Protein
EM	Expectation Maximisation
FCS	Fluorescence Correlation Spectroscopy
FIFO	First-In First-Out
FISH	Fluorescence in-situ Hybridisation
FLIM	Fluorescence Lifetime Imaging Microscopy
FRAP	Fluorescence Recovery After Photobleaching
FRET	Fluorescence Resonance Energy Transfer
GA	Genetic Algorithm
GCBLs	Graph Cut Based Level Set
GFP	Green Fluorescent Protein
GLCM	Gray Level Co-occurrence Matrix
GMM	Gaussian Mixture Modelling
GRF	Gibbs Random Field
HLF	Highest Level First
ICC	Immunocytochemistry
ICF	Immunocytofluorescence
ICM	Iterated Conditional Modes
IHC	Immunohistochemistry
IHF	Immunohistofluorescence
IOD	Integrated Optical Density
Laser	Light Amplification by Stimulated Emission of Radiation
LBP	Loopy Belief Propagation
LED	Light Emitting Diode
LoG	Laplacian of Gaussian
MAP	Maximum A Posteriori
MIS	Medical Image Segmentation

MLP	Multi-Layered Perceptron
MRF	Markov Random Field
MST	Minimum Spanning Tree
NA	Numerical Aperture
ORI	Optimised Rotational Invariance
OTF	Optical Transfer Function
PSF	Point Spread Function
RF	Random Field
RNA	Ribonucleic Acid
SNR	Signal-to-Noise Ratio
TV	Total Variation
UV	Ultraviolet

For/Dedicated to/To my...

Chapter 1

Introduction

1.1 Literature Review

The Literature Review is here.

1.2 Outline and Contributions

The introduction is here.

1.3 Thesis Overview

The remainder of the thesis outline.

Chapter ?? is where we cover the mathematical foundation to Graph Cut image segmentation.

Chapter ?? is where we cover the mathematical foundation to Graph Cut image segmentation.

Chapter ?? is where we cover the mathematical foundation to Graph Cut image segmentation.

Chapter ?? is where we cover the mathematical foundation to Graph Cut image segmentation.

Chapter 2 is where we cover the mathematical foundation to Graph Cut image segmentation.

Chapter ?? is where we cover the mathematical foundation to Graph Cut image segmentation.

Chapter ?? concludes the thesis with suggestions for further work.

Chapter 2

Parameter Estimation for ACWE Chan-Vese Segmentation

[Introduction] What is special about the Chan-Vese formulation to the Mumford-Shah evolution energy function. Advantages, disadvantages (parameter estimation). Course of the chapter.

2.1 Graph Cut Model for Chan-Vese Segmentation

Chan-Vese formulation of the Mumford-Shah formulation. Length approximation using discrete representations (cut-metrics). Discrete representation of Chan-Vese formulation. Graph representation and sub-modularity constraint. Insensitivity to initialisation. What do the parameters mean and how do they influence the final result. In this section we briefly reintroduce the graph cut formulation for the Chan-Vese formulation of the Mumford-Shah evolution energy function for image segmentation. The Mumford-Shah model uses gradient descent techniques to obtain a minimum but as previously discussed, ??, they usually terminate at local minima. By reformulating the energy function in a discrete form that allows for appropriate graph representability, we can use graph cuts, which are able to terminate at a global minimum, to iteratively converge to the optimal solution. For an in-depth exposition into this technique, look to [13, 38, 66].

The level set representation of the Mumford-Shah energy function is

$$\begin{aligned}
 F(c_1, c_2, \phi) = & \mu \int_{\Omega} \delta(\phi(x, y)) |\nabla \phi(x, y)| dx dy \\
 & + \nu \int_{\Omega} H(\phi(x, y)) dx dy \\
 & + \lambda_1 \int_{\Omega} |u(x, y) - c_1|^2 H(\phi(x, y)) dx dy \\
 & + \lambda_2 \int_{\Omega} |u(x, y) - c_2|^2 (1 - H(\phi(x, y))) dx dy,
 \end{aligned} \tag{2.1}$$

where $u(x, y)$ is the image, $H(\cdot)$ is the Heaviside step function, $\delta(\cdot)$ is the Dirac delta function, $\phi : \Omega \rightarrow \mathbb{R}$ is the level set function, such that:

$$\begin{aligned}
 \omega &= \{(x, y) \in \Omega | \Phi(x_p) > 0\} \text{ Inside the boundary} \\
 \bar{\omega} &= \{(x, y) \in \Omega | \Phi(x_p) < 0\} \text{ Outside the boundary} \\
 C = \partial\omega &= \{(x, y) \in \Omega | \Phi(x_p) = 0\} \text{ Along the boundary,}
 \end{aligned} \tag{2.2}$$

c_1 and c_2 are the arithmetic means given by:

$$c_1(\phi) = \frac{\int_{\Omega} u(x, y) H(\phi(x, y)) dx dy}{\int_{\Omega} H(\phi(x, y)) dx dy}, \quad (2.3)$$

$$c_2(\phi) = \frac{\int_{\Omega} u(x, y) (1 - H(\phi(x, y))) dx dy}{\int_{\Omega} (1 - H(\phi(x, y))) dx dy}. \quad (2.4)$$

The piecewise smooth approximation of the image is then

$$u(x, y) = c_1 H(\phi(x, y)) + c_2 (1 - H(\phi(x, y))). \quad (2.5)$$

Discrete Approximation of Contour Length For the energy function to be represented as a graph, one of the requirements is that it must be in a discrete representation. This means that the length of the contour, the first term in Equation (2.1), must be approximated discretely and be graph representable. This work has already been done by Kolmogorov and Boykov in [67, 68] where they used the Cauchy-Crofton theorem. The theorem states that the length of a curve can be approximated by draw a large number of straight lines from 0 to 2π and counting the number of intersections between the lines and the contour. The mathematical representation is

$$\int_L n_L dL = \int_0^\pi \int_{-\infty}^\infty n_L d\rho d\theta = 2\|C\|_E, \quad (2.6)$$

where n_L is the number of intersections between the contour C and the line L , $\|C\|_E$ is the Euclidean length of the contour, $0 < \rho < \infty$ and $0 < \theta < 2\pi$. From this the discrete approximation used by Boykov and Zabih is

$$\|C\|_E = \frac{1}{2} \sum_k n_k \frac{\delta^2 \Delta \theta_k}{|e_k|} = \frac{1}{2} \sum_k n_k w_k \quad (2.7)$$

An example of approximating the contour by two grids is illustrated in Figure 2.1(a) using four families of parallel lines which are 45° apart.

Discrete Representation of Mumford-Shah Function With the exception of the second term in Equation (2.1), the remaining terms are represented easily discretely. For each pixel $p \in \Omega$, let x_p be a binary variable such that

$$x_p = \begin{cases} 0 & \phi(p) \leq 0 \\ 1 & \phi(p) > 0 \end{cases} \quad (2.8)$$

The means can now be calculated using

$$c_1 = \frac{\sum_p u(x, y) x_p}{\sum_p x_p}, \quad (2.9)$$

$$c_2 = \frac{\sum_p u(x, y) (1 - x_p)}{\sum_p (1 - x_p)}. \quad (2.10)$$

For simplification, $\nu = 0$. To determine contour length using an 8-neighbourhood system, as illustrated in Figure 2.1(b), we set $\Delta\rho = 1$. The weight w_k is assigned to it's corresponding edge e_k . The Euclidean length of the edges is $|e_1| = |e_3| = 1$ and $|e_2| = |e_4| = \sqrt{2}$, therefore

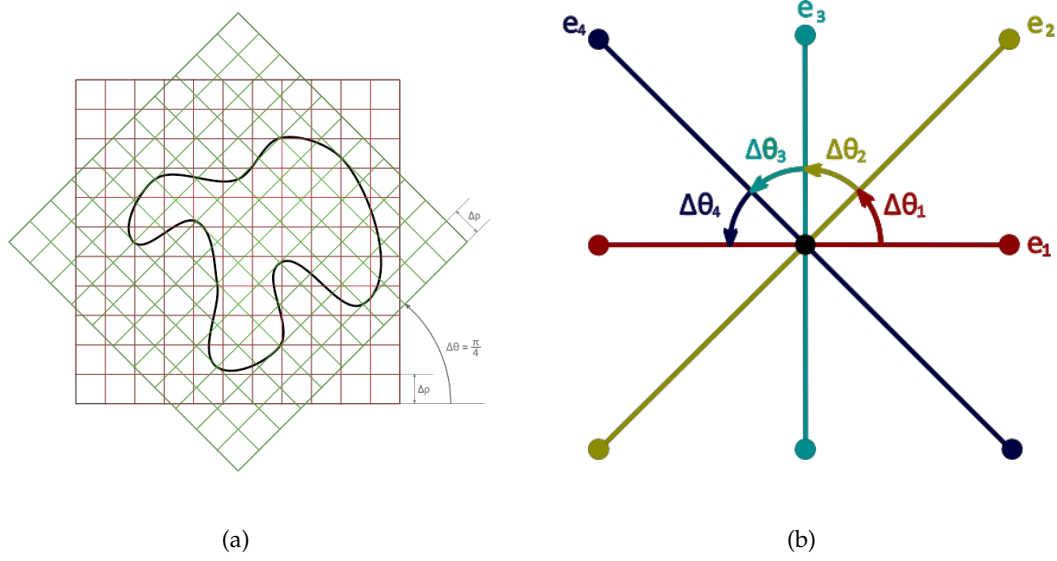


FIGURE 2.1: (a) Cauchy-Crofton length approximation. (b) 8-connected neighbourhood system.

the corresponding weights, which are determined using Equation (2.7), is $w_1 = w_3 = \frac{\pi}{8}$ and $w_2 = w_4 = \frac{\pi}{8\sqrt{2}}$. To calculate n_k we need to count the intersections between the lines and the contour. An intersection between two pixels p and q exists *if and only if* x_p and x_q have different labels.

$$n_k = x_p(1 - x_q) + x_q(1 - x_p); k = (pq) \in \mathcal{N}_p. \quad (2.11)$$

The contour length can now fully be expressed discretely as

$$\|C\|_E = \sum_{p,q \in e_k} w_k(x_p(1 - x_q) + x_q(1 - x_p)). \quad (2.12)$$

The discrete representation of Equation (2.1) is

$$\begin{aligned} F(x_1, \dots, x_n) = & \mu \sum_{p,q \in e_k} w_k(x_p(1 - x_q) + x_q(1 - x_p)) \\ & + \lambda_1 \sum_p |u(x, y) - c_1|^2 x_p \\ & + \lambda_2 \sum_p |u(x, y) - c_2|^2 (1 - x_p) \end{aligned} \quad (2.13)$$

Graph Representation The discrete energy function Equation (2.13) has been shown that it obey the submodularity constraint for graph representability. Therefore the data energy and regularisation energy is

$$E^p(x_p) = \lambda_1 |u(x, y) - c_1|^2 x_p + \lambda_2 |u(x, y) - c_2|^2 (1 - x_p) \quad (2.14)$$

$$E^{pq}(x_p, x_q) = (x_p + x_q - 2x_p x_q) w_{pq} \quad (2.15)$$

The graph for the energy function is constructed as in [42].

2.2 Modified Weighting and Parameter Estimation

What is wrong with the previously described graph weighting. What would we expect from a better weighting system.

2.2.1 Graph Weighting

The first thing we do is normalise the weighting for both the data and smoothing connections. For the weighting of the neighbourhood connections we use the Euclidean distance between adjacent nodes. This results in neighbourhood connections as illustrated in Figure 2.2. The range of pixel intensities is also normalised i.e. $p \in [0, 1]$. The weight of the connection from the source to the node p is given by $E^i(0)|_{i=p} = \lambda_0 |p - c_0|^2$. This is seen as how far away the pixel is from c_0 . Similarly, the weight of the connection from the node to the sink is given by $E^i(1)|_{i=p} = \lambda_1 |p - c_1|^2$, i.e. how far away the pixel is from c_1 . The fully connected graph for a single node in the 8-connected neighbourhood system is illustrated in Figure 2.2.

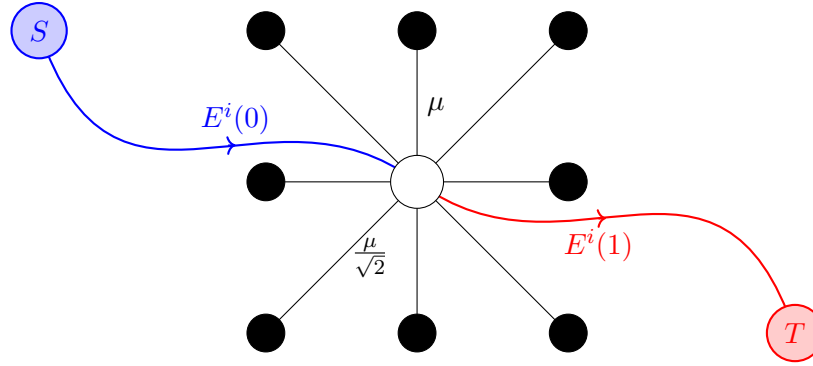


FIGURE 2.2: Fully connected single node.

Describe the modified weighting and parameter relations.

2.2.2 Analysis of Weighting System and Parameter Relationships

Describe the relationship between various parameters including their limits and ranges.

To better understand the relationship between λ_0 and λ_1 and its impact on the final solution we explicitly formalise the dependency and set

$$\lambda_0 = \alpha \lambda_1. \quad (2.16)$$

Forcing this relation between λ_0 and λ_1 makes further analysis simpler and more intuitive. We can immediately see a constraint on α . Since, we require data connections to be positive, i.e. $E^i(0), E^i(1) \geq 0$ (SEE SECTION??), this gives us a lowerbound on α for positive concavity of the energy functions

$$\alpha > 0 \text{ lowerbound on } \alpha \quad (2.17)$$

We will now analyse the flow through a single node. We use Figure 2.2 to facilitate our explanation. From the neighbourhood connections, in an 8-connected neighbourhood construction, the maximum flow into or out of a node to its neighbours is

$$f_{max} = 4\mu + 4\frac{\mu}{\sqrt{2}} = \mu \left(2\sqrt{2} + 4 \right). \quad (2.18)$$

To guarantee that a node will be place in the set with mean c_0 we know that the incoming flow from the source must completely saturate all flow outlets, this can be expressed as

$$E^i(0) > E^i(1) + \mu \left(2\sqrt{2} + 4 \right). \quad (2.19)$$

This can be read as "*The source saturates the sink and all neighbourhood connections*". Similarly to guarantee the node will be in the set with mean c_1

$$E^i(1) > E^i(0) + \mu \left(2\sqrt{2} + 4 \right). \quad (2.20)$$

This can be read as "*The sink is larger than the source and all neighbourhood connections*". To aid in understanding the energies we use Figure 2.3.

For quadratic energies with $0 < c_0 < c_1 < 1$, there is a point, between c_0 and c_1 , where the incoming flow from the source is completely saturates the sink with no excess remaining. This point, where the energies are equal, we call p_e , i.e. $E_0(p_e) = E_1(p_e)$. This point of zero net flow can be found as follows

$$\begin{aligned} E^{i=p_e}(1) &= E^{i=p_e}(0) \\ \lambda_1(p_e - c_1)^2 &= \lambda_0(p_e - c_0)^2 \\ \frac{(p_e - c_0)^2}{(p_e - c_1)^2} &= \frac{\lambda_1}{\lambda_0} \\ \frac{p_e - c_0}{p_e - c_1} &= \sqrt{\frac{\lambda_1}{\lambda_0}} \quad \text{or} \quad \frac{p_e - c_0}{p_e - c_1} = -\sqrt{\frac{\lambda_1}{\lambda_0}} \end{aligned}$$

We know that

$$\begin{aligned} c_0 &< p_e < c_1 \\ \therefore p_e - c_0 &> 0 \quad \text{and} \quad p_e - c_1 < 0 \end{aligned}$$

It follows, directly , that

$$\begin{aligned} \frac{p_e - c_1}{p_e - c_0} &= -\sqrt{\frac{\lambda_1}{\lambda_0}} \\ \frac{(p_e - c_0) + (c_0 - c_1)}{p_e - c_0} &= -\sqrt{\frac{\lambda_1}{\lambda_0}} \\ \frac{c_0 - c_1}{p_e - c_0} &= -\left(\sqrt{\frac{\lambda_1}{\lambda_0}} + 1 \right) \\ p_e &= c_0 + \frac{c_1 - c_0}{\sqrt{\frac{\lambda_1}{\lambda_0}} + 1} \end{aligned}$$

After substituting the relation in Equation (2.16) we get

$$p_e = c_0 + \frac{c_1 - c_0}{\sqrt{\alpha} + 1} \quad (2.21)$$

The point where the energies are equal, p_e , is shown in Figure 2.3.

Analysis of the relationship between p_e and α From Equation (2.21) we note that there is one

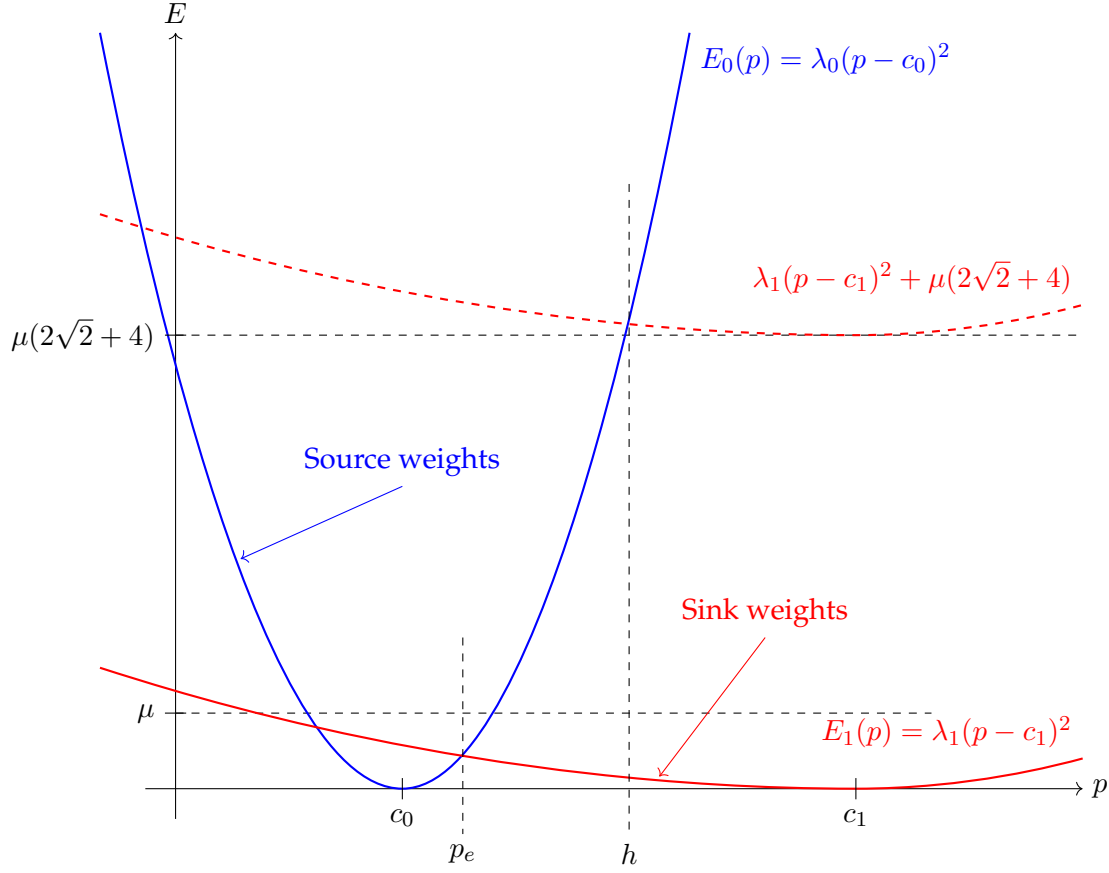
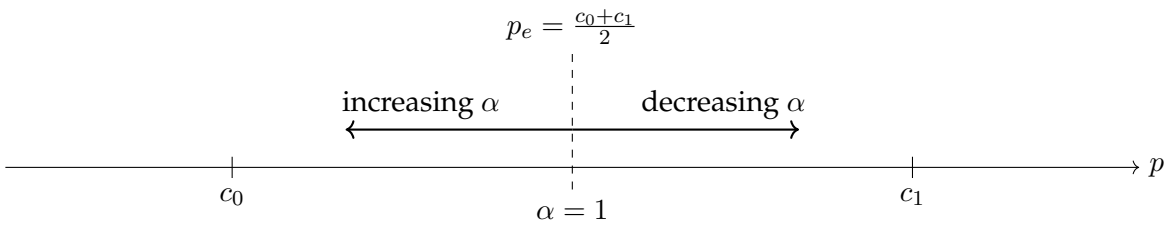


FIGURE 2.3: Data energy functions plot.

tunable parameter, i.e. α . We can see that p_e and α are inversely related. This is expressed mathematically as

$$\begin{aligned} \text{if } \alpha = 1, p_e &= c_0 + \frac{c_1 - c_0}{1 + \sqrt{1}} = \frac{c_0 + c_1}{2} && \text{(midpoint between } c_0 \text{ and } c_1) \\ \lim_{\alpha \rightarrow \infty} p_e &= \lim_{\alpha \rightarrow \infty} c_0 + \frac{c_1 - c_0}{1 + \sqrt{1}} = c_0 && \text{(maximum } \alpha \text{ yields lowerbound on } p_e) \\ \lim_{\alpha \rightarrow 0} p_e &= \lim_{\alpha \rightarrow 0} c_0 + \frac{c_1 - c_0}{1 + \sqrt{0}} = c_1 && \text{(minimum } \alpha \text{ yields upperbound on } p_e) \end{aligned}$$

The relationship between p_e and α is illustrated in Figure 2.4.

FIGURE 2.4: Relationship between α and p_e .

Figuring α If we are able to make good estimates on p_e , c_0 and c_1 for the final segmented image, then it is possible to calculate α as follows:

$$\begin{aligned} p_e &= c_0 + \frac{c_1 - c_0}{\sqrt{\alpha} + 1} \\ 1 + \sqrt{\alpha} &= \frac{c_1 - c_0}{p_e - c_0} \\ \alpha &= \left(\frac{c_1 - c_0}{p_e - c_0} - 1 \right)^2 \end{aligned} \quad (2.22)$$

Lowerbound on μ When we found the point, p_e , where the energies are equal in Equation (2.21), we ignored the other solution as it was not within the range from c_0 to c_1 . Let this point be p_{e^*} . If this point is positive and $0 < p_{e^*} < c_0$ then we must ensure that at no point within this range that the source flow saturates all the outgoing edges. This force a limit on how low μ can be. This is only of significant concern when $\alpha > 1$. We only need to concern ourselves with the point $p = 0$ as this is the point where the difference $E^i(0) - E^i(1)$ is the largest. The lowerbound on μ can be obtained as follows

$$\begin{aligned} E^i(0)|_{p_i=0} &< E^i(1)|_{p_i=0} + \mu (2\sqrt{2} + 4) \\ \lambda_0 c_0^2 &< \lambda_1 c_1^2 + \mu (2\sqrt{2} + 4) \\ \therefore \mu (2\sqrt{2} + 4) &> \lambda_0 c_0^2 - \lambda_1 c_1^2 \\ \mu &> \frac{\lambda_0 c_0^2 - \lambda_1 c_1^2}{(2\sqrt{2} + 4)} \end{aligned}$$

Taking into account the relation in Equation (2.16) this becomes

$$\mu > \frac{\lambda_1(\alpha c_0^2 - c_1^2)}{(2\sqrt{2} + 4)} \quad (2.23)$$

Absolutely in the source set From Equation (2.19) we can see that there is a point beyond which all nodes which correspond to pixel value higher than that point will be saturated and have excess flow which means that they will be in the source set. We will call this point the *saturation point* and denote it by h . This is shown in Figure 2.3. This point can be determined as follows:

$$\begin{aligned} \lambda_0(h - c_0)^2 &> \lambda_1(h - c_1)^2 + f_{max} \\ \lambda_0(h - c_0)^2 - \lambda_1(h - c_1)^2 &> f_{max} \\ (\lambda_0 - \lambda_1)h^2 + (-2\lambda_0 c_0 + 2\lambda_1 c_1)h + (\lambda_0 c_0^2 - \lambda_1 c_1^2 - f_{max}) &> 0 \end{aligned}$$

The solutions to h are

$$h = \frac{(2\lambda_0 c_0 - 2\lambda_1 c_1) \pm \sqrt{(-2\lambda_0 c_0 + 2\lambda_1 c_1)^2 - 4(\lambda_0 - \lambda_1)(\lambda_0 c_0^2 - \lambda_1 c_1^2 - f_{max})}}{2(\lambda_0 - \lambda_1)}$$

Substituting the relation in Equation (2.16)

$$\begin{aligned} h &= \frac{(\alpha c_0 - c_1) \pm \sqrt{(c_1 - \alpha c_0)^2 - (\alpha - 1)(\alpha c_0^2 - c_1^2 - \frac{f_{max}}{\lambda_1})}}{\alpha - 1} \\ &= \frac{(\alpha c_0 - c_1) \pm \sqrt{\alpha(c_0 - c_1)^2 + \frac{f_{max}}{\lambda_1}(\alpha - 1)}}{\alpha - 1} \end{aligned}$$

If the μ is greater than the lowerbound in Equation (2.23) then there is only one solution to h which is of importance. This is the positive solution for h which is

$$h = \frac{(\alpha c_0 - c_1) + \sqrt{\alpha(c_0 - c_1)^2 + \frac{\mu(2\sqrt{2}+4)}{\lambda_1}(\alpha - 1)}}{\alpha - 1} \quad (2.24)$$

This point is marked off in Figure 2.3.

Determining λ_1 Given good approximations for c_0, c_1, α, h and μ , we can calculate the appropriate value for λ_1 . We proceed from Equation (2.19) as follows

$$\begin{aligned} \lambda_0(h - c_0)^2 &= \lambda_1(h - c_1)^2 + \mu(2\sqrt{2} + 4) \\ \lambda_1(\alpha(h - c_0)^2 - (h - c_1)^2) &= \mu(2\sqrt{2} + 4) \\ \lambda_1 &= \frac{\mu(2\sqrt{2} + 4)}{\alpha(h - c_0)^2 - (h - c_1)^2} \end{aligned} \quad (2.25)$$

The parameter estimation is based on the assumption that sufficiently good approximations for c_0, c_1, p_e and h can be obtained. From these approximation we calculate the approximation for α using Equation (2.22). The parameters μ and α are related and aren't seperable, therefore we set choose to set μ . We can then calculate λ_1 using Equation (2.25). For the chosen μ we can calculate the upperbound on α to ensure that the constraint Equation (2.23) is met. The constraint on λ_1 is calculated as follows

$$\begin{aligned} \mu(2\sqrt{2} + 4) &> \lambda_1(\alpha c_0^2 - c_1^2) \\ \lambda_1 &< \frac{\mu(2\sqrt{2} + 4)}{\alpha c_0^2 - c_1^2} \end{aligned} \quad (2.26)$$

Finally λ_0 can be calculated using Equation (2.16).

2.2.3 Tuning Parameters for Fluorescence Microscopy

What sort of image properties are we tuning for? E.g. dark bg, low contrast, etc. Parameters limits and ranges.

2.3 Experimental Results

Present and analyse the experimental results.

Appendix A

Introduction to Graph Theory

Graph A graph G is a pair (V, E) , where V is the set of nodes/vertices and E is the set of edges consisting of pairs (u, v) where $u, v \in V$. The graph is assumed to be finite i.e. $|V| = n$ and $|E| = m$.

In an **undirected graph**, the edge (u, v) and (v, u) are not distinct. That is, they refer to the same edge. However, in a **directed graph**, the two edge are now distinct. In a directed graph with edge (u, v) , u is known as the **tail** and v is known as the **head**. In directed graphs, edges, also known as arcs, are depicted by placing arrowheads at the head of the edge. Given an edge $e = (u, v)$, u and v are said to be **incident** on e . A graph is said to be **simple** if it does not contain any self-loops. A **self-loop** is an edge with its end points being the same vertex.

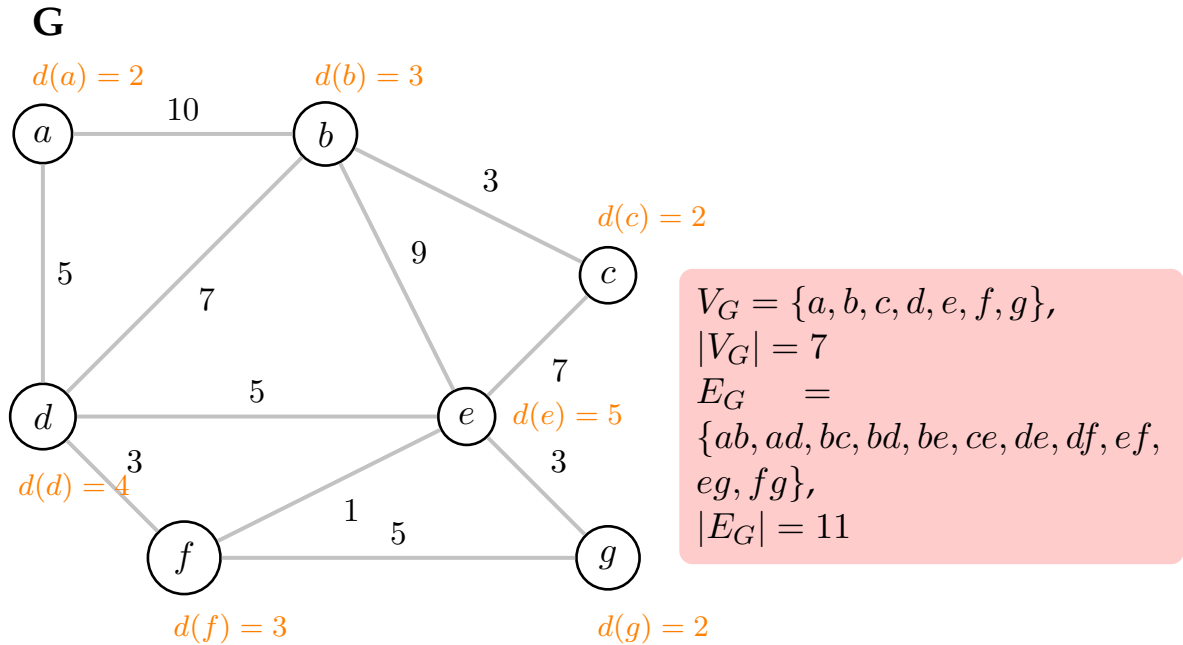


FIGURE A.1: Undirected weighted graph **G**. The degree of each node is shown next to the corresponding node. The graph is simple. The red box shows the vertex set, V_G , and edge set, E_G , and their corresponding norm.

Degree The degree of a vertex v is the number of edges incident on it. $\deg(v) = |\{(u, v), (v, u) \in E\}|$. A self-loop counts for 2.

If a graph is directed, also known as a **digraph**, then a node v has an **in-degree** $d_{in}(v)$ and an **out-degree** $d_{out}(v)$. A digraph is said to be **balanced** if $d_{in}(v) = d_{out}(v), \forall v \in V$.

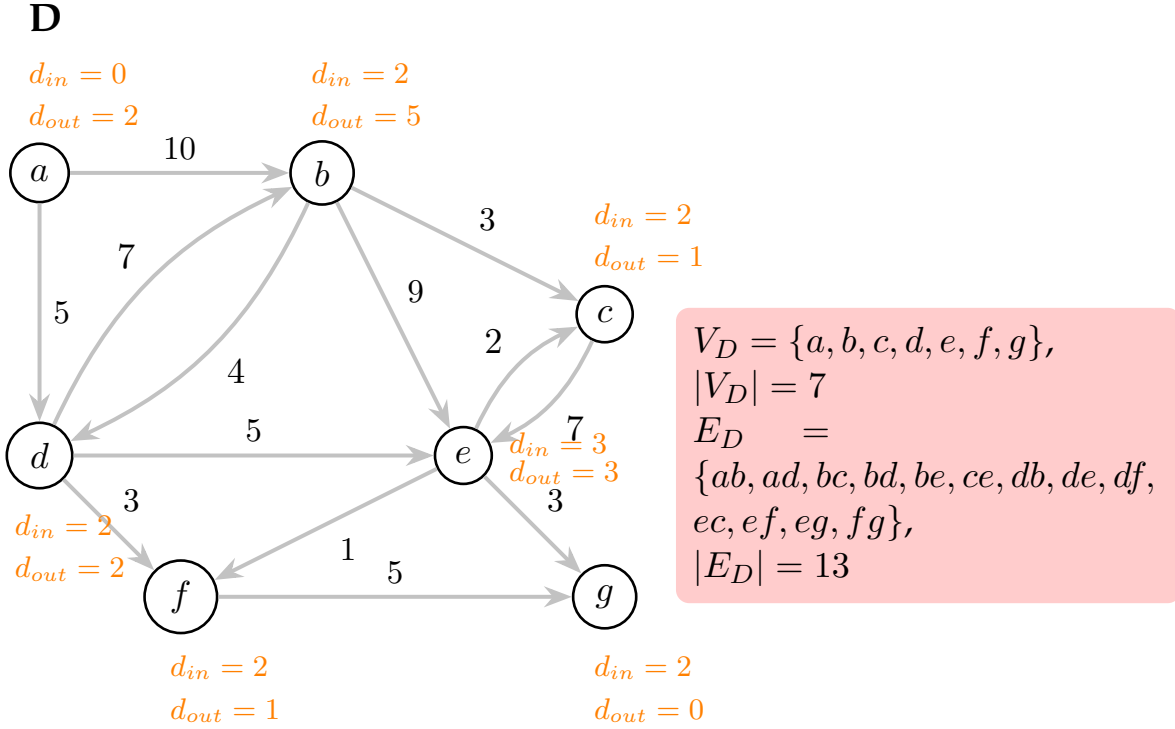


FIGURE A.2: Directed weighted graph (Digraph) **D**. The in-degree and out-degree is shown next to each node. The graph is simple and not balanced. The red box shows the vertex set, V_D , and edge set, E_D , and their corresponding norm.

Subgraph A graph $G' = (V', E')$ is said to be a sub-graph of $G = (V, E)$, denoted as $G' \subseteq G$, if $V' \subseteq V$ and $E' \subseteq E$.

Clique A clique is a maximal subgraph.

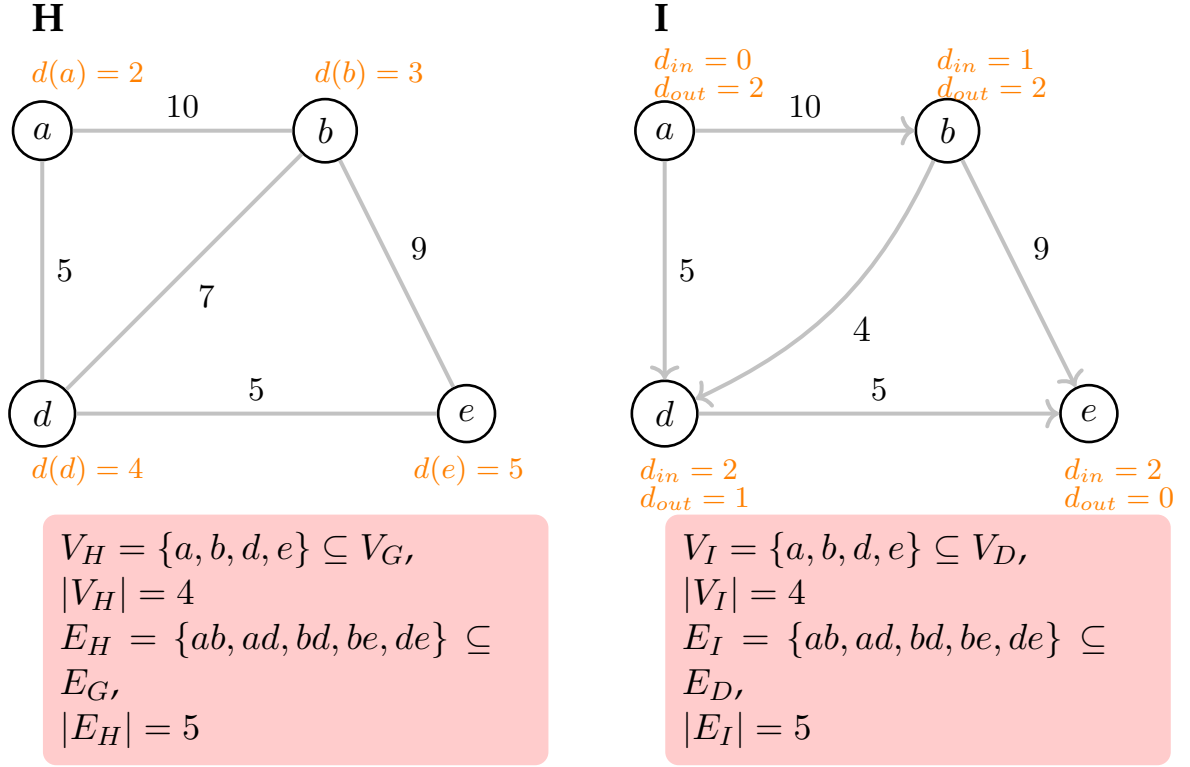


FIGURE A.3: Undirected weighted graph **H** is a subgraph of **G** in Figure XX, $H \subseteq G$. Directed weighted graph **I** is a subgraph of **D** in Figure XX, $I \subseteq D$. The degree of each node is shown next to the corresponding node. The red box shows the vertex set, the edge set and their corresponding norms.

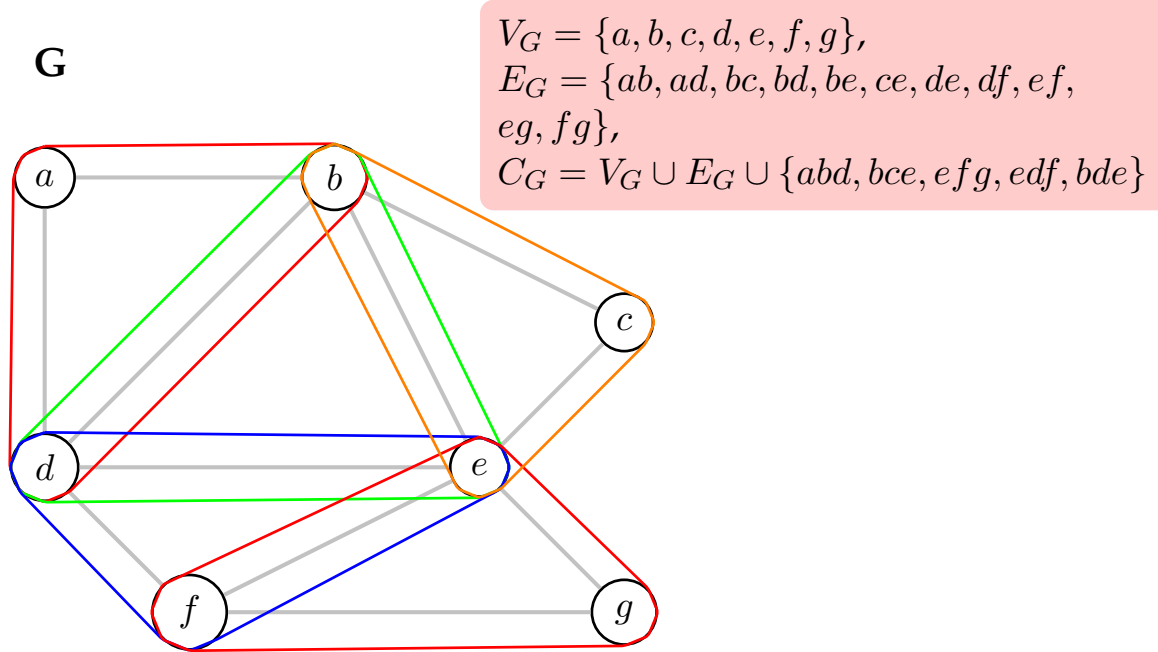


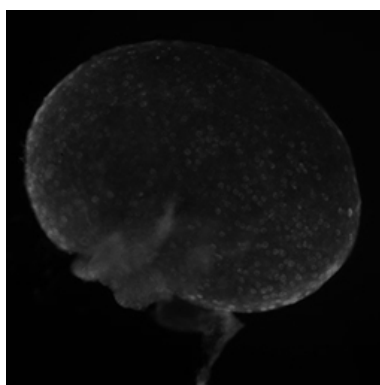
FIGURE A.4: Cliques of the undirected weighted graph **G**. The maximal cliques are shown by the hyperedges that encompass the nodes of that clique.

Appendix B

Cell Images Dataset

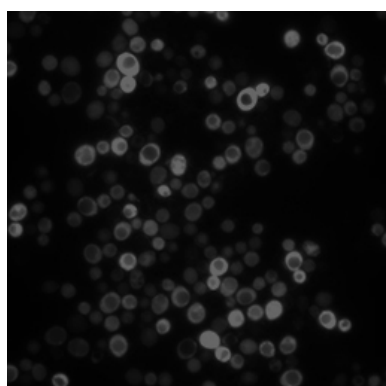
This dataset is compiled to represent the type of variations of cell images obtained in fluorescence microscopy.

B.1 Test Data

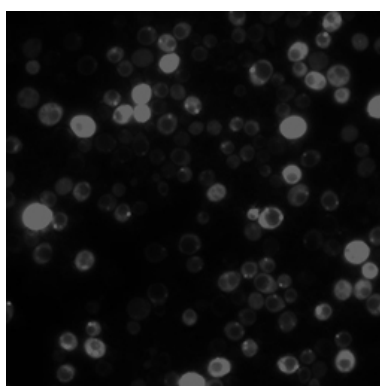


(a)

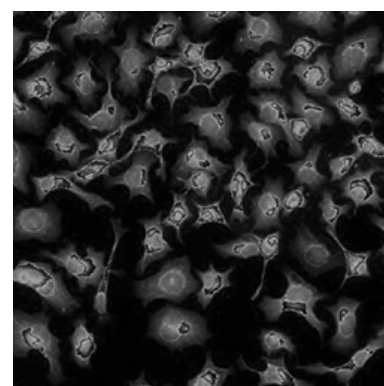
FIGURE B.1: Uneven Illumination



(a)



(b)



(c)

FIGURE B.2: High cell density

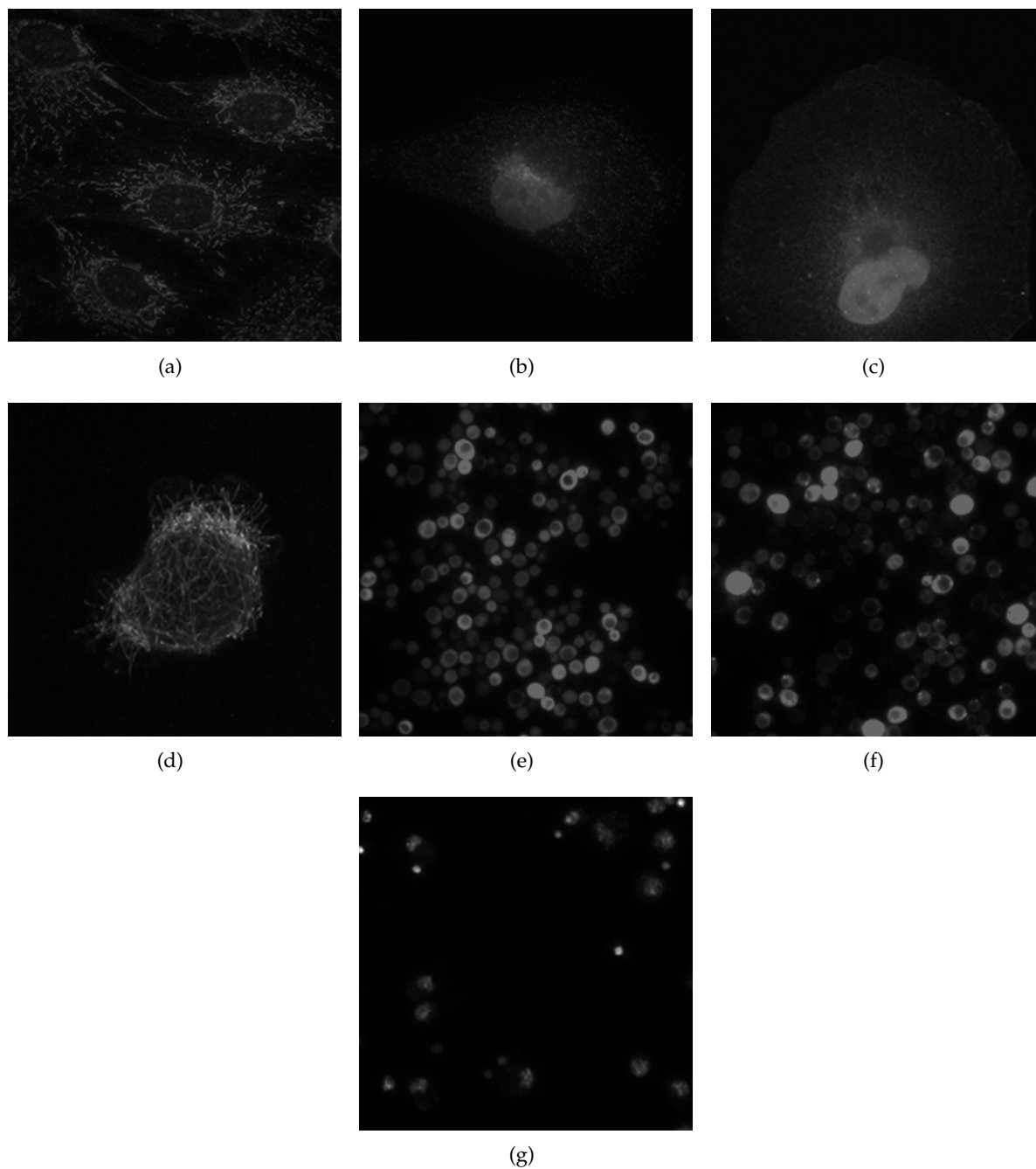


FIGURE B.3: Multi-modal (non-bi-modal)

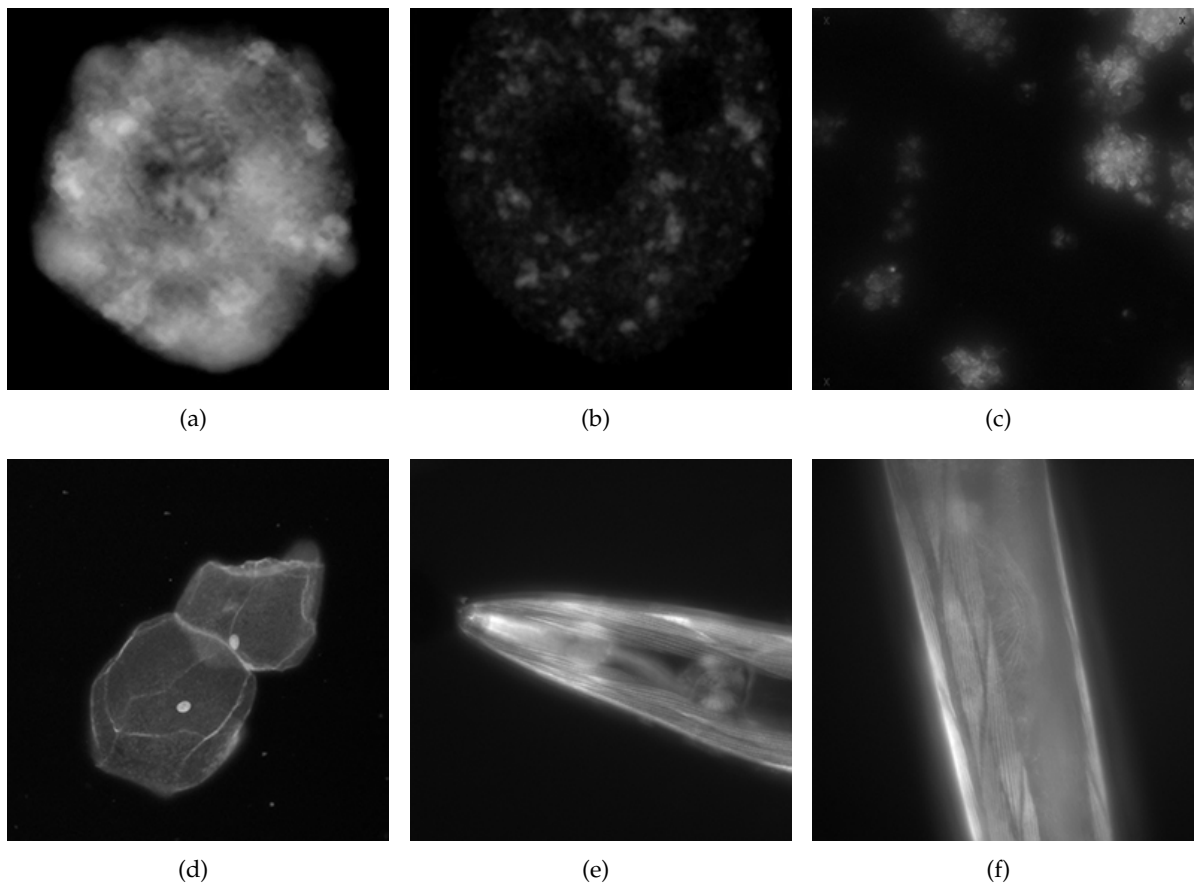


FIGURE B.4: Hazy/Glowing Edges

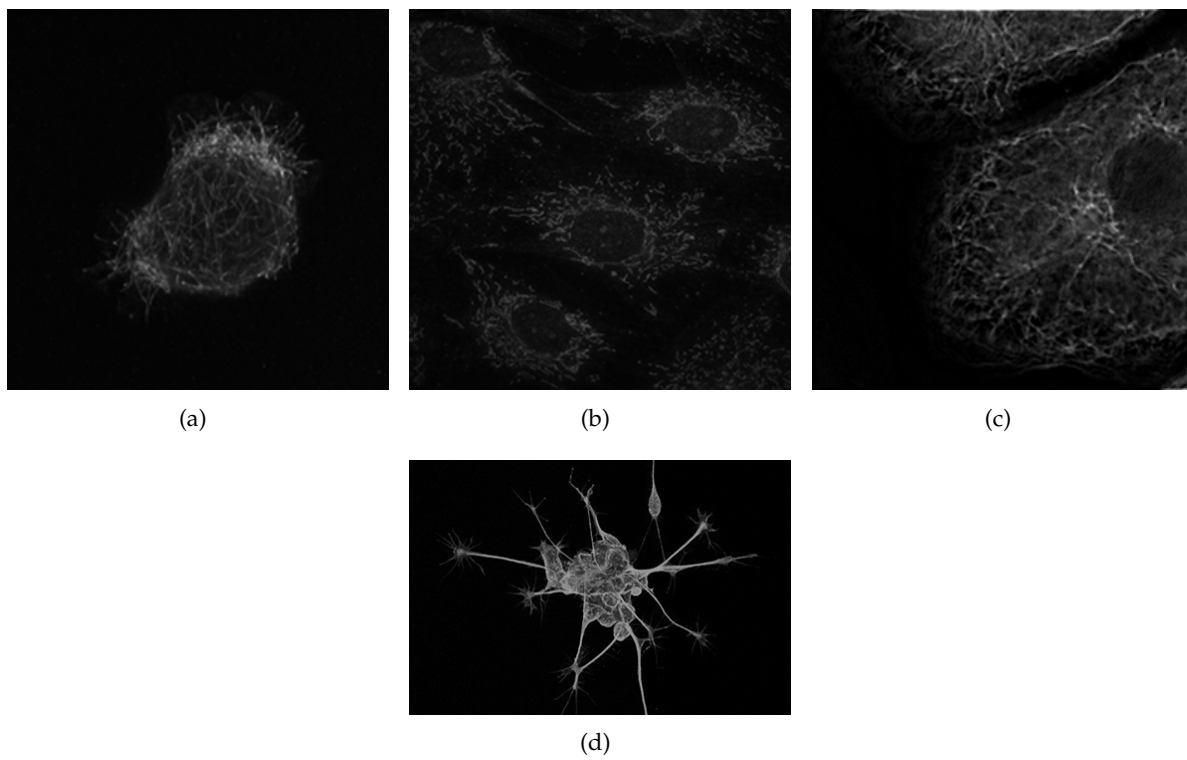


FIGURE B.5: Thin Tentacles

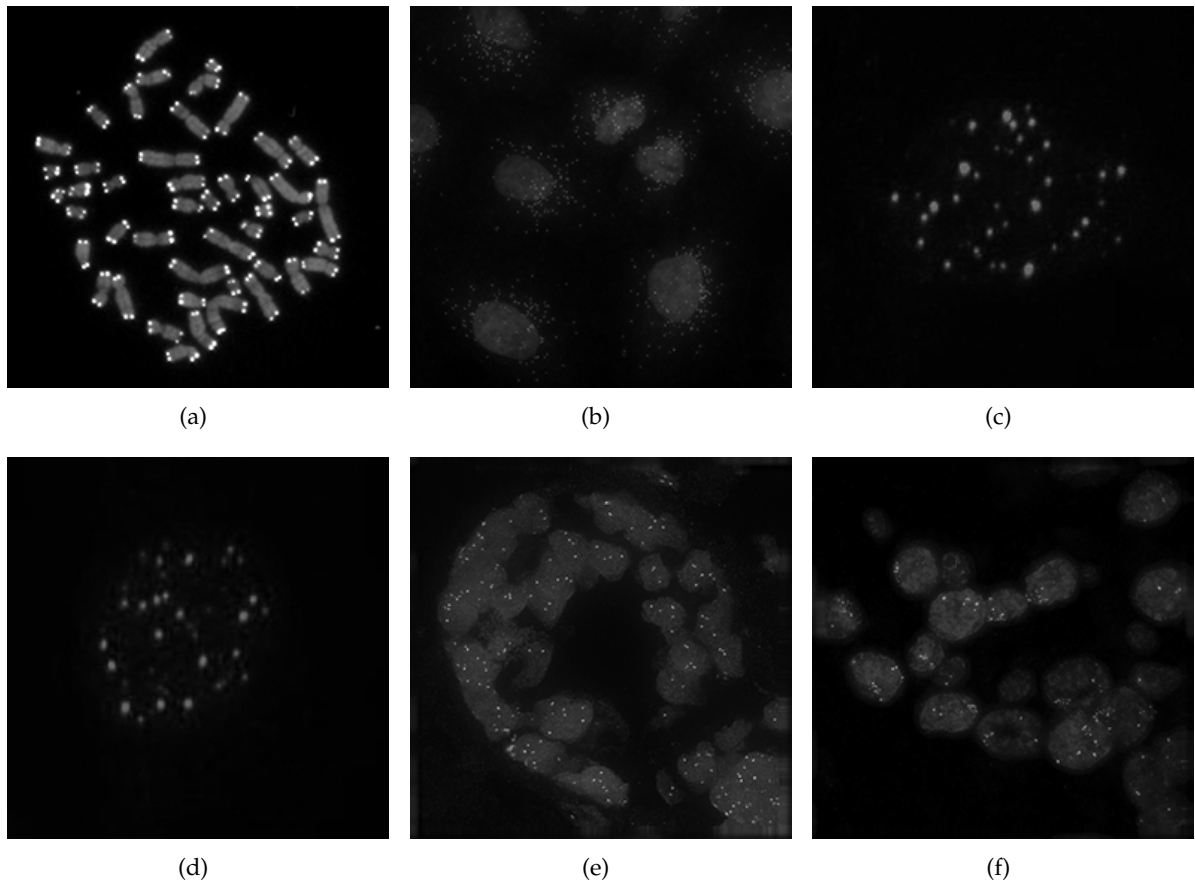
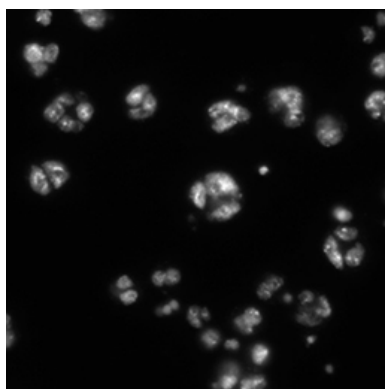
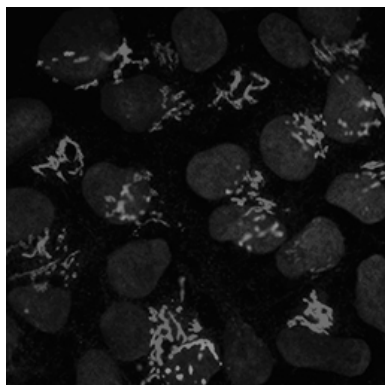


FIGURE B.6: Bright Spots and Speckles



(a)



(b)

FIGURE B.7: To ben categorised

Bibliography

- [1] Tomaso Poggio, Vincent Torre, and Christof Koch. "Computational vision and regularization theory". In: *Nature* 317.6035 (1985), pp. 314–319. DOI: [10.1038/317314a0](https://doi.org/10.1038/317314a0). URL: <http://dx.doi.org/10.1038/317314a0>.
- [2] D. Terzopoulos. "Regularization of Inverse Visual Problems Involving Discontinuities". In: *IEEE Transactions on Pattern Analysis and Machine Intelligence* PAMI-8.4 (1986), pp. 413–424. ISSN: 0162-8828. DOI: [10.1109/TPAMI.1986.4767807](https://doi.org/10.1109/TPAMI.1986.4767807).
- [3] S.I. Kabanikhin. "Definitions and examples of inverse and ill-posed problems". In: *J. Inv. Ill-Posed Problems* 16 (2008), pp. 317–357. ISSN: 0162-8828. DOI: [10.1515/JIIP.2008.069](https://doi.org/10.1515/JIIP.2008.069).
- [4] Albert Tarantola. *Inverse Problem Theory and Methods and Models for Parameter Estimation*. Philadelphia, PA, USA: Society for Industrial and Applied Mathematics, 2005, pp. 1–37. ISBN: 0-89871-572-5.
- [5] Mario Bertero and Patrizia Boccacci. *Introduction to Inverse Problems in Imaging*. Bath, UK: IOP Publishing Ltd, 1998, pp. 1–37. ISBN: 0 7503 0439 1.
- [6] M. Bertero and M. Piana. "Inverse problems in biomedical imaging: modeling and methods of solution". In: *Complex Systems in Biomedicine*. Ed. by Alfio Quarteroni, Luca Formaggia, and Alessandro Veneziani. Milano: Springer Milan, 2006, pp. 1–33. ISBN: 978-88-470-0396-5. DOI: [10.1007/88-470-0396-2_1](https://doi.org/10.1007/88-470-0396-2_1). URL: http://dx.doi.org/10.1007/88-470-0396-2_1.
- [7] Andrew Thomas Delong. "Advances in Graph-Cut Optimization: Multi-Surface Models, Label Costs, and Hierarchical Costs [online]". Doctoral theses, Dissertations. The University of Western Ontario, London Ontario, Canada, 2011 [cit. 2016-09-19]. URL: <http://www.psi.toronto.edu/~andrew/papers/thesis.pdf>.
- [8] David Waltz. "Understanding Line Drawings of Scenes with Shadows". In: *The Psychology of Computer Vision*. McGraw-Hill, 1975, pp. 19–91.
- [9] Azriel Rosenfeld, Robert A. Hummel, and Steven W. Zucker. "Definitions and examples of inverse and ill-posed problems". In: *IEEE Transactions on Systems, MAN, and Cybernetics* 6.6 (1976), pp. 420–433.
- [10] Katsuhiko Sakaue, Akira Amano, and Naokazu Yokoya. "Optimization Approaches in Computer Vision and Image Processing". In: *IEECE Trans. Inf. & Syst.* E82.3 (1999), pp. 534–547.
- [11] Yuri Boykov, Olga Veksler, and Ramin Zabih. "Fast Approximate Energy Minimization via Graph Cuts". In: *IEEE Trans. Pattern Anal. Mach. Intell.* 23.11 (2001), pp. 1222–1239. ISSN: 0162-8828. DOI: [10.1109/34.969114](https://doi.org/10.1109/34.969114). URL: <http://dx.doi.org/10.1109/34.969114>.
- [12] Vladimir Kolmogorov. "Convergent Tree-Reweighted Message Passing for Energy Minimization". In: *Proc. Int'l Workshop Artificial Intelligence and Statistics*. 2005.

- [13] David Mumford. "Optimal approximation by piecewise smooth functions and associated variational problems". In: *Commun. Pure Applied Mathematics* (1989), pp. 577–685.
- [14] Jianbo Shi and Jitendra Malik. "Normalized Cuts and Image Segmentation". In: *IEEE Transactions on Pattern Analysis and Machine Intelligence* 22 (1997), pp. 888–905.
- [15] T. Athanasiadis et al. "Semantic Image Segmentation and Object Labeling". In: *IEEE Transactions on Circuits and Systems for Video Technology* 17.3 (2007), pp. 298–312. ISSN: 1051-8215. DOI: [10.1109/TCSVT.2007.890636](https://doi.org/10.1109/TCSVT.2007.890636).
- [16] Robert J. Adler and Jonathan E. Taylor. *Random fields and geometry*. Springer monographs in mathematics. New York: Springer, 2007. ISBN: 978-0-387-48112-8. URL: <http://opac.inria.fr/record=b1123290>.
- [17] Anatoly V. Skorokhod Iosif I. Gikhman. *Introduction to the Theory of Random Processes*. Dover Books on Mathematics. Dover Publications, 1996. ISBN: 0486693872.
- [18] Matthew Brett, Will Penny, and Stefan Kiebel. *An Introduction to Random Field Theory*. MRC Cognition and Brain Sciences Unit, Cambridge UK, 2003.
- [19] Richard L. Smith. "Introduction to Besag (1974) Spatial Interaction and the Statistical Analysis of Lattice Systems". In: *Breakthroughs in Statistics*. Ed. by Samuel Kotz and Norman L. Johnson. New York, NY: Springer New York, 1997, pp. 285–323. ISBN: 978-1-4612-0667-5. DOI: [10.1007/978-1-4612-0667-5_13](https://doi.org/10.1007/978-1-4612-0667-5_13). URL: http://dx.doi.org/10.1007/978-1-4612-0667-5_13.
- [20] Stuart Geman and Donald Geman. "Stochastic Relaxation, Gibbs Distributions, and the Bayesian Restoration of Images". In: *IEEE Trans. Pattern Anal. Mach. Intell.* 6.6 (1984), pp. 721–741. ISSN: 0162-8828. DOI: [10.1109/TPAMI.1984.4767596](https://doi.org/10.1109/TPAMI.1984.4767596). URL: <http://dx.doi.org/10.1109/TPAMI.1984.4767596>.
- [21] Julian Besag. "On the statistical analysis of dirty pictures". In: *Journal of the Royal Statistical Society B* 48.3 (1986), pp. 48–259.
- [22] John Lafferty. "Conditional random fields: Probabilistic models for segmenting and labeling sequence data". In: Morgan Kaufmann, 2001, pp. 282–289.
- [23] J. M. Hammersley and P. E. Clifford. "Markov random fields on finite graphs and lattices". In: Unpublished manuscript (1971).
- [24] Gerhard Winkler. *Image Analysis, Random Fields and Markov Chain Monte Carlo Methods: A Mathematical Introduction (Stochastic Modelling and Applied Probability)*. Secaucus, NJ, USA: Springer-Verlag New York, Inc., 2006. ISBN: 3540442138.
- [25] Cyril Cassisa. "Local Vs Global Energy Minimization Methods: Application to Stereo Matching". In: *IEEE* (2010), pp. 678–683. ISSN: 978-1-4244-6789-1.
- [26] Olga Veksler. "Efficient Graph-based Energy Minimisation Methods in Computer Vision [online]". Doctoral theses, Dissertations. Cornell University, 1999 [cit. 2016-09-20]. URL: <http://www.csd.uwo.ca/faculty/olga/Papers/thesis.pdf>.
- [27] V. Černý. "Thermodynamical approach to the traveling salesman problem: An efficient simulation algorithm". In: *Journal of Optimization Theory and Applications* 45.1 (1985), pp. 41–51. ISSN: 1573-2878. DOI: [10.1007/BF00940812](https://doi.org/10.1007/BF00940812). URL: <http://dx.doi.org/10.1007/BF00940812>.
- [28] S. Kirkpatrick, C. D. Gelatt, and M. P. Vecchi. "Optimization by simulated annealing". In: *SCIENCE* 220.4598 (1983), pp. 671–680.

- [29] L. A. MacEachern and T. Manku. "Genetic algorithms for active contour optimization". In: *Circuits and Systems, 1998. ISCAS '98. Proceedings of the 1998 IEEE International Symposium on*. Vol. 4. 1998, pp. 229–232. DOI: [10.1109/ISCAS.1998.698801](https://doi.org/10.1109/ISCAS.1998.698801).
- [30] Lucia Ballerini. "Genetic Snakes for Medical Images Segmentation". In: *Evolutionary Image Analysis, Signal Processing and Telecommunications: First European Workshops, EvoIASP'99 and EuroEcTel'99, Göteborg, Sweden, May 26-27, 1999. Proceedings*. Ed. by Riccardo Poli et al. Berlin, Heidelberg: Springer Berlin Heidelberg, 1999, pp. 59–73. ISBN: 978-3-540-48917-7. DOI: [10.1007/10704703_5](https://doi.org/10.1007/10704703_5). URL: http://dx.doi.org/10.1007/10704703_5.
- [31] Lucia Ballerini. "Genetic Snakes for Color Images Segmentation". In: *Applications of Evolutionary Computing: EvoWorkshops 2001: EvoCOP, EvoFlight, EvoIASP, EvoLearn, and EvoS-TIM Como, Italy, April 18–20, 2001 Proceedings*. Ed. by Egbert J. W. Boers. Berlin, Heidelberg: Springer Berlin Heidelberg, 2001, pp. 268–277. ISBN: 978-3-540-45365-9. DOI: [10.1007/3-540-45365-2_28](https://doi.org/10.1007/3-540-45365-2_28). URL: http://dx.doi.org/10.1007/3-540-45365-2_28.
- [32] Reinhard Möller and Rene Zeipelt. "Automatic Segmentation of 3D-MRI Data Using a Genetic Algorithm". In: *Medical Imaging and Augmented Reality: First International Workshop, MIAR 2001, Hong Kong, China, June 10-12, 2001. Proceedings*. 2001, pp. 278–281. DOI: [10.1109/MIAR.2001.930303](https://doi.org/10.1109/MIAR.2001.930303). URL: <http://dx.doi.org/10.1109/MIAR.2001.930303>.
- [33] O. Ibáñez et al. "Genetic approaches for topological active nets optimization". In: *Pattern Recognition* 42.5 (2009), pp. 907–917. ISSN: 0031-3203. DOI: [http://dx.doi.org/10.1016/j.patcog.2008.09.005](https://doi.org/10.1016/j.patcog.2008.09.005). URL: <http://www.sciencedirect.com/science/article/pii/S0031320308003762>.
- [34] Chris McIntosh and Ghassan Hamarneh. "Medical Image Segmentation: Energy Minimization and Deformable Models (Chapter 23)". In: *Medical Imaging: Technology and Applications* (2013). Ed. by T. Farncombe and K. Iniewski, pp. 661–692. URL: <http://www.cs.sfu.ca/~hamarneh/ecopy/crc2013a.pdf>.
- [35] D. Terzopoulos. "On matching deformable models to images". In: *Optical Society of America, Topical Meeting on Machine Vision*. Provided by the SAO/NASA Astrophysics Data System. 1987. URL: <http://adsabs.harvard.edu/abs/1980osa..meet..160T>.
- [36] Michael Kass, Andrew Witkin, and Demetri Terzopoulos. "Snakes: Active contour models". In: *International Journal of Computer Vision* 1.4 (1988), pp. 321–331.
- [37] Vicent Caselles, Ron Kimmel, and Guillermo Sapiro. "Geodesic Active Contours". In: *International Journal of Computer Vision* 22.1 (1997), pp. 61–79. ISSN: 0920-5691. DOI: [10.1023/A:1007979827043](https://doi.org/10.1023/A:1007979827043). URL: <http://dx.doi.org/10.1023/A:1007979827043>.
- [38] T. F. Chan and L. A. Vese. "Active Contours Without Edges". In: *Trans. Img. Proc.* 10.2 (2001), pp. 266–277. ISSN: 1057-7149. DOI: [10.1109/83.902291](https://doi.org/10.1109/83.902291). URL: <http://dx.doi.org/10.1109/83.902291>.
- [39] Judea Pearl. *Probabilistic Reasoning in Intelligent Systems: Networks of Plausible Inference*. San Francisco, CA, USA: Morgan Kaufmann Publishers Inc., 1988. ISBN: 0-934613-73-7.
- [40] Brendan Frey and David MacKay. "A Revolution: Belief Propagation in Graphs With Cycles". In: *In Neural Information Processing Systems*. MIT Press, 1998, pp. 479–485.

- [41] William T. Freeman, Egon C. Pasztor, and Owen T. Carmichael. "Learning Low-Level Vision". In: *Int. J. Comput. Vision* 40.1 (2000), pp. 25–47. ISSN: 0920-5691. DOI: [10.1023/A:1026501619075](https://doi.org/10.1023/A:1026501619075). URL: <http://dx.doi.org/10.1023/A:1026501619075>.
- [42] Vladimir Kolmogorov and Ramin Zabih. "What energy functions can be minimized via graph cuts?" In: *IEEE Transactions on Pattern Analysis and Machine Intelligence* 26.2 (2004), pp. 65–81.
- [43] Y. Boykov and M.P. Jolly. "Interactive graph cuts for optimal boundary and region segmentation of objects in N-D images". In: *Proc. IEEE Int'l Conf. on Computer Vision* 1 (2001), pp. 105–112.
- [44] Yuri Boykov and Vladimir Kolmogorov. "An Experimental Comparison of Min-Cut/Max-Flow Algorithms for Energy Minimization in Vision". In: *IEEE Transactions on Pattern Analysis and Machine Intelligence* 26 (2001), pp. 359–374.
- [45] Vladimir Kolmogorov et al. "A Comparative Study of Energy Minimization Methods for Markov Random Fields with Smoothness-Based Priors". In: *IEEE Transactions on Pattern Analysis & Machine Intelligence* 30.undefined (2007), pp. 1068–1080. ISSN: 0162-8828. DOI: doi.ieeecomputersociety.org/10.1109/TPAMI.2007.70844.
- [46] P. Kohli, M. Pawan Kumar, and P. H. S. Torr. "P³ & Beyond: Move Making Algorithms for Solving Higher Order Functions". In: *IEEE Transactions on Pattern Analysis and Machine Intelligence* 31.9 (2009), pp. 1645–1656. ISSN: 0162-8828. DOI: [10.1109/TPAMI.2008.217](https://doi.org/10.1109/TPAMI.2008.217).
- [47] Nikos Komodakis, Georgios Tziritas, and Nikos Paragios. "Fast, Approximately Optimal Solutions for Single and Dynamic MRFs". In: *CVPR*. IEEE Computer Society, 2007. ISBN: 1-4244-1179-3. URL: <http://dblp.uni-trier.de/db/conf/cvpr/cvpr2007.html#KomodakisTP07>.
- [48] M. Pawan Kumar and Daphne Koller. "MAP Estimation of Semi-metric MRFs via Hierarchical Graph Cuts". In: *Proceedings of the Twenty-Fifth Conference on Uncertainty in Artificial Intelligence*. UAI '09. Arlington, Virginia, United States: AUAI Press, 2009, pp. 313–320. ISBN: 978-0-9749039-5-8. URL: <http://dl.acm.org/citation.cfm?id=1795114.1795151>.
- [49] D. M. Greig, B. T. Porteous, and A. H. Seheult. "Exact Maximum A Posteriori Estimation for Binary Images". In: *Journal of the Royal Statistical Society. Series B (Methodological)* 51.2 (1989), pp. 271–279. ISSN: 00359246. URL: <http://www.jstor.org/stable/2345609>.
- [50] Sébastien Roy and Ingemar Johansson Cox. "A maximum-flow formulation of the n-camera stereo correspondence problem". In: *Computer Vision, 1998. Sixth International Conference on*. 1998, pp. 492–499.
- [51] Yuri Boykov, Olga Veksler, and Ramin Zabih. "Markov Random Fields with Efficient Approximations." In: *CVPR*. IEEE Computer Society, 1998, pp. 648–655. ISBN: 0-8186-8497-6. URL: <http://dblp.uni-trier.de/db/conf/cvpr/cvpr1998.html#BoykovVZ98>.
- [52] L. R. Ford and D. R. Fulkerson. "Maximal Flow through a Network". In: *Canadian Journal of Mathematics* 8 (1956), pp. 399–404. URL: <http://www.rand.org/pubs/papers/P605/>.
- [53] E.A. Dinic. "Algorithm for solution of a problem of maximum flow in a network with power estimation". In: *Soviet Math* 11 (1970), pp. 1277–1280.

- [54] Jack Edmonds and Richard M. Karp. "Theoretical Improvements in Algorithmic Efficiency for Network Flow Problems". In: *J. ACM* 19.2 (1972), pp. 248–264. ISSN: 0004-5411. DOI: [10.1145/321694.321699](https://doi.org/10.1145/321694.321699). URL: <http://doi.acm.org/10.1145/321694.321699>.
- [55] Andrew V. Goldberg and Robert E. Tarjan. "A New Approach to the Maximum-flow Problem". In: *J. ACM* 35.4 (1988), pp. 921–940. ISSN: 0004-5411. DOI: [10.1145/48014.61051](https://doi.org/10.1145/48014.61051). URL: <http://doi.acm.org/10.1145/48014.61051>.
- [56] Narsingh Deo. *Graph Theory with Applications to Engineering and Computer Science (Prentice Hall Series in Automatic Computation)*. Upper Saddle River, NJ, USA: Prentice-Hall, Inc., 1974. ISBN: 0133634736.
- [57] John Adrian Bondy. *Graph Theory With Applications*. Oxford, UK, UK: Elsevier Science Ltd., 1976. ISBN: 0444194517.
- [58] Maarten van Steen. *Graph theory and complex networks : An introduction*. Lexington: Maarten van Steen, 2010. ISBN: 978-90-815406-1-2. URL: <http://opac.inria.fr/record=b1130915>.
- [59] Mark Newman. *Networks: An Introduction*. 1st edition. Oxford University Press, 2010. ISBN: 0199206651.
- [60] Eugene Lawler. "4.5. Combinatorial Implications of Max-Flow Min-Cut Theorem, 4.6. Linear Programming Interpretation of Max-Flow Min-Cut Theorem". In: *Combinatorial Optimization: Networks and Matroids*. Ed. by Eugene Lawler. Dover, 2001, pp. 117–120. ISBN: 0-486-41453-1.
- [61] Solomon Eyal Shimony. "Finding MAPs for belief networks is NP-hard". In: *Artificial Intelligence* 68.2 (1994), pp. 399–410. ISSN: 0004-3702. DOI: [http://dx.doi.org/10.1016/0004-3702\(94\)90072-8](http://dx.doi.org/10.1016/0004-3702(94)90072-8). URL: <http://www.sciencedirect.com/science/article/pii/0004370294900728>.
- [62] Thomas H. Cormen et al. *Introduction to Algorithms, Third Edition*. 3rd. The MIT Press, 2009. ISBN: 0262033844, 9780262033848.
- [63] V. B. Cherkassky and V. A. Goldberg. "On Implementing the Push—Relabel Method for the Maximum Flow Problem". In: *Algorithmica* 19.4 (19), pp. 390–410. ISSN: 1432-0541. DOI: [10.1007/PL00009180](https://doi.org/10.1007/PL00009180). URL: <http://dx.doi.org/10.1007/PL00009180>.
- [64] R. Szeliski et al. "A Comparative Study of Energy Minimization Methods for Markov Random Fields with Smoothness-Based Priors". In: *IEEE Transactions on Pattern Analysis and Machine Intelligence* 30.6 (2008), pp. 1068–1080. ISSN: 0162-8828. DOI: [10.1109/TPAMI.2007.70844](https://doi.org/10.1109/TPAMI.2007.70844).
- [65] Nhat Bao Sinh Vu. "Image Segmentation with Semantic Priors: A Graph Cut Approach [online]". Doctoral theses, Dissertations. University of California, Santa Barbara, 2008 [cit. 2016-10-03]. URL: <https://vision.ece.ucsb.edu/sites/vision.ece.ucsb.edu/files/publications/NhatsThesis.pdf>.
- [66] Noha El Zehiry et al. "Graph Cut Optimization for the Mumford-Shah Model". In: *The Seventh IASTED International Conference on Visualization, Imaging and Image Processing*. VIIP '07. Palma de Mallorca, Spain: ACTA Press, 2007, pp. 182–187. ISBN: 978-0-88986-692-8. URL: <http://dl.acm.org/citation.cfm?id=1659167.1659203>.

- [67] Vladimir Kolmogorov and Yuri Boykov. “What Metrics Can Be Approximated by Geo-Cuts, Or Global Optimization of Length/Area and Flux.” In: *ICCV*. IEEE Computer Society, 2005, pp. 564–571. ISBN: 0-7695-2334-X. URL: <http://dblp.uni-trier.de/db/conf/iccv/iccv2005-1.html#KolmogorovB05>.
- [68] Yuri Boykov. “Computing geodesics and minimal surfaces via graph cuts”. In: *in International Conference on Computer Vision*. 2003, pp. 26–33.